

Why must a solar forcing be larger than a CO<sub>2</sub> forcing to cause the same global mean surface temperature change?

This content has been downloaded from IOPscience. Please scroll down to see the full text.

2016 Environ. Res. Lett. 11 044013

(<http://iopscience.iop.org/1748-9326/11/4/044013>)

View [the table of contents for this issue](#), or go to the [journal homepage](#) for more

Download details:

IP Address: 14.139.128.19

This content was downloaded on 09/06/2016 at 07:55

Please note that [terms and conditions apply](#).

## Environmental Research Letters



## LETTER

Why must a solar forcing be larger than a CO<sub>2</sub> forcing to cause the same global mean surface temperature change?

## OPEN ACCESS

## RECEIVED

18 January 2016

## REVISED

27 February 2016

## ACCEPTED FOR PUBLICATION

11 March 2016

## PUBLISHED

7 April 2016

Angshuman Modak<sup>1</sup>, Govindasamy Bala<sup>1,2</sup>, Long Cao<sup>3</sup> and Ken Caldeira<sup>4</sup><sup>1</sup> Divecha Center for Climate Change and Center for Atmospheric and Oceanic Sciences, Indian Institute of Science, Bangalore 560012, India<sup>2</sup> Interdisciplinary center for water research, Indian Institute of Science, Bangalore-12, India<sup>3</sup> School of Earth Sciences, Zhejiang University, Hangzhou, Zhejiang 310027, People's Republic of China<sup>4</sup> Department of Global Ecology, Carnegie Institution for Science, Stanford, CA 94305, USAE-mail: [amatcaos@caos.iisc.ernet.in](mailto:amatcaos@caos.iisc.ernet.in)**Keywords:** radiative forcing, efficacy, climate feedback, fast cloud adjustments, rapid land surface warmingSupplementary material for this article is available [online](#)

Original content from this work may be used under the terms of the [Creative Commons Attribution 3.0 licence](#).

Any further distribution of this work must maintain attribution to the author(s) and the title of the work, journal citation and DOI.

**Abstract**

Many previous studies have shown that a solar forcing must be greater than a CO<sub>2</sub> forcing to cause the same global mean surface temperature change but a process-based mechanistic explanation is lacking in the literature. In this study, we investigate the physical mechanisms responsible for the lower efficacy of solar forcing compared to an equivalent CO<sub>2</sub> forcing. Radiative forcing is estimated using the Gregory method that regresses top-of-atmosphere (TOA) radiative flux against the change in global mean surface temperature. For a 2.25% increase in solar irradiance that produces the same long term global mean warming as a doubling of CO<sub>2</sub> concentration, we estimate that the efficacy of solar forcing is ~80% relative to CO<sub>2</sub> forcing in the NCAR CAM5 climate model. We find that the fast tropospheric cloud adjustments especially over land and stratospheric warming in the *first four months* cause the slope of the regression between the TOA net radiative fluxes and surface temperature to be steeper in the solar forcing case. This steeper slope indicates a stronger net negative feedback and hence correspondingly a larger solar forcing than CO<sub>2</sub> forcing for the same equilibrium surface warming. Evidence is provided that rapid land surface warming in the first four months sets up a land-sea contrast that markedly affects radiative forcing and the climate feedback parameter over this period. We also confirm the robustness of our results using simulations from the Hadley Centre climate model. Our study has important implications for estimating the magnitude of climate change caused by volcanic eruptions, solar geoengineering and past climate changes caused by change in solar irradiance such as Maunder minimum.

**1. Introduction**

The concept of radiative forcing was introduced to estimate the equilibrium temperature change that would occur as a result of changes in the radiatively active agents such as atmospheric greenhouse gases, aerosols, land cover and solar irradiance (Hansen *et al* 1997, 2005). Understanding the response of the climate system to changes in these radiative forcing agents is fundamental in projecting future climate change. Many definitions and variants on the basic radiative forcing have been provided (Hansen *et al* 2005, Myhre *et al* 2013) but they are all closely

related to the top-of-atmosphere (TOA) imbalance that occurs soon after radiatively active agents are introduced. The radiative forcing concept has played a central role in the concept of Global Warming Potentials and CO<sub>2</sub>-equivalence of radiative forcing agents (Myhre *et al* 2013), and thus has played a central role in climate policy discussions. However, under existing definitions of radiative forcings including the effective radiative forcing (Forster *et al* 2013; table S1), different forcing agents with the same radiative forcing could result in different global mean climate responses (Hansen *et al* 1997, 2005), thus undermining in part the

fundamental rationale for using the radiative forcing concept.

To address this issue, the concept of ‘efficacy’ of radiative forcing has been introduced (Hansen *et al* 2005). The efficacy of a radiative forcing mechanism is defined to be the ratio of equilibrium global mean temperature change that would be produced by per unit forcing by an agent relative to the equilibrium temperature change that would be caused by per unit CO<sub>2</sub> forcing from the same initial climate state (Hansen *et al* 2005). The concept of ‘efficacy’ could be used to develop better estimates of ‘CO<sub>2</sub>-equivalence’ and thus could contribute to developing efficient strategies for reducing amounts of climate change (Hansen *et al* 2005).

Past studies (Hansen *et al* 2005) have shown that forcing agents such as black carbon aerosols have smaller efficacy (i.e., less than one) while others such as methane have larger efficacy (i.e., greater than one). Several other studies (Forster *et al* 2000, Hansen *et al* 2005, Lambert and Faull 2007, Bala *et al* 2010, Schmidt *et al* 2012) have shown that the efficacy of the solar radiative forcing is less than one. For example, a recent multi-model study (Schmidt *et al* 2012) finds that the efficacy of solar forcing ranges from 0.72 to 0.85 across four different state-of-the-art earth system models that participated in The Geoengineering Model Intercomparison project. Differences in convective cloud feedbacks (Forster *et al* 2000) and rapid adjustments of the troposphere (Lambert and Faull 2007) have been attributed to the smaller efficacy of the solar radiative forcing. However, these studies do not provide a mechanistic understanding of how cloud feedbacks or the rapid tropospheric adjustments cause a smaller efficacy of solar forcing relative to the CO<sub>2</sub> forcing.

In this paper, we use climate model simulations to re-visit the efficacy of solar forcing relative to equivalent CO<sub>2</sub> forcing. We adopt the recently developed framework (Andrews *et al* 2009, Dong *et al* 2009, Bala *et al* 2010, Cao *et al* 2011, Cao *et al* 2012, Staten *et al* 2014, Cao *et al* 2015) of decomposing the total response into two components: ‘fast adjustment’ and ‘slow response or feedback’. The fast adjustment refers to the changes in the thermal structure of the atmosphere and related variables such as water vapor and clouds before a change in global-mean surface temperature, and the slow response or feedback refers to changes that occurs in response to changes in surface temperature. However, it is important to recognize that there is no clear separation of fast adjustment and slow response as the evolution of climate change is a continuous process (Cao *et al* 2015). In this paper, therefore, we use the term ‘feedback’ to refer to changes in radiative fluxes on all timescales as long as the units are W m<sup>-2</sup> K<sup>-1</sup> while the term ‘adjustment’ is used to refer to changes in state variables such as temperature and clouds in the first few months. We note that in some studies such as Held *et al* (2010) the fast

component is defined as a response of the climate system to an abrupt forcing at a time scale of a few years, when the sea surface temperature is allowed to change.

We use the Gregory method to estimate the radiative forcing as the intercept of the regression between the net radiative flux change at TOA versus the change in the global mean surface temperature (Gregory *et al* 2004). Our aim is to develop a mechanistic understanding of the physical mechanisms and adjustment processes that are responsible for any difference in the efficacy between solar and CO<sub>2</sub> forcing. We discuss the evolution of the climate response to solar and CO<sub>2</sub> forcing on the timescales of days to weeks to months, which is somewhat similar to several previous studies (Dong *et al* 2009, Cao *et al* 2012, Kamae and Watanabe 2012). For instance, Cao *et al* (2012) investigated the fast adjustments due to abrupt increase in the solar irradiance and atmospheric CO<sub>2</sub> on a timescale of few days and showed that the fast adjustments in the troposphere leads to a suppression of precipitation in the CO<sub>2</sub> case but not in the solar case. While the focus of that study (Cao *et al* 2012) was characterizing the response of the surface energy budget and the hydrological cycle on the timescale of days to weeks, here we focus on a mechanistic explanation of the response of the net radiative fluxes at TOA during the first 4 months after the forcings are imposed. This mechanistic explanation contributes to the understanding of how differing feedbacks in this time period leads to different efficacy for solar forcing and CO<sub>2</sub> forcing.

We demonstrate that the total climate change in mixed layer climate change simulations can be divided into three time periods governed by different dominant processes. After the forcing is introduced, the *first period* lasts about one week which can be considered as ‘ultrafast response’, and is dominated by atmospheric adjustments to pre-existing surface temperature patterns. In the case of a CO<sub>2</sub> increase, this period introduces a suppression of global mean precipitation which is absent in the case of solar irradiance increase (Cao *et al* 2012). The *second period* extends to about four months after the introduction of the radiative agent, and is dominated by fast adjustments of the stratosphere and land surface. For CO<sub>2</sub> and solar irradiance increases, the resulting change in land-sea temperature contrast increases the atmospheric flow from ocean to land in the lower troposphere. The concomitant increase in upward atmospheric motion over land and downward motion over the ocean in the troposphere causes changes to cloud properties and extent which have substantial radiative consequences. During this period the stratosphere cools in the CO<sub>2</sub> forcing case but it warms in the solar case. The *third period* extends out decades and centuries—the ‘slow response’ when the dominant process is the adjustment of sea-surface temperature, in which ocean processes play important roles (Bala *et al* 2010, Andrews *et al* 2009, Cao *et al* 2015). However, we caution that there is no sharp distinction of these time periods as

the evolution of climate change is continuous and hence there are overlaps between these processes (Cao *et al* 2015).

## 2. Model and experiments

We use the Community Atmosphere Model, CAM5 (Neale *et al* 2010) developed by the National Center for Atmospheric Research (NCAR). It is coupled to the Community Land Model CLM4 and a slab ocean (thermodynamic mixed-layer) model with a thermodynamic sea ice model. In this model, the depth of the slab ocean varies spatially with the depth in the tropics ranging between 10 and 30 m, while in high latitudes it varies from 10 m to a specified cap of 200 m. The mixed-layer ocean model is a simplification of the full ocean model but it is useful to study climate change on decadal time scales as the mixed layer ocean adjusts on decadal timescales before the deep ocean has time to respond. The horizontal resolution is  $1.9^\circ \times 2.5^\circ$  (latitude  $\times$  longitude) and there are 30 vertical levels for the atmosphere (model top is at  $\sim 3.5$  hPa). The model's vertical coordinate is a hybrid sigma-pressure system with upper levels in pressure coordinates and lower levels in sigma coordinates which is a terrain following coordinate (Neale *et al* 2010). Relative to the earlier version of the model CAM4 that has a climate sensitivity (global mean warming for a doubling of  $\text{CO}_2$ ) of 3.2 K, CAM5 has a larger sensitivity of 4.0 K. The higher sensitivity of CAM5 is associated with more positive cloud feedbacks and larger  $\text{CO}_2$  radiative forcing (Gettelman *et al* 2012).

We have performed a set of three simulations: (i) a control 'CTL', with a  $\text{CO}_2$  concentration of 284.7 ppmv (pre-industrial value) and an incoming solar flux of  $1360 \text{ W m}^{-2}$ , (ii) '2x $\text{CO}_2$ ', with doubled atmospheric  $\text{CO}_2$  concentration (569.4 ppmv) and a solar constant of  $1360 \text{ W m}^{-2}$ , and (iii) 'SOLAR' with a  $\text{CO}_2$  concentration that is same as in CTL but solar insolation increased by 2.25% to  $1390.6 \text{ W m}^{-2}$ . Summary of the experiments is shown in tables S2 and S3. The increase in solar irradiance is applied throughout the solar spectral region in the model which ranges from 120 nm to 99 975 nm. The 2.25% increase in the solar irradiance is chosen such that this amount of increase in solar irradiance yields similar long term change in the global mean surface temperature to that in 2x $\text{CO}_2$ . We have applied the forcings as a step function change at the start of the simulations.

The above set of three experiments are performed in two different configurations: (i) The fixed-sea surface temperature (SST) simulations where the SST and the sea-ice extent is prescribed and held fixed, and (ii) Slab Ocean Model (SOM) simulations which is the full atmosphere and thermodynamic mixed-layer ocean mode. The fixed-SST simulations are run for 40 years and the last 20 years are used to compute the effective radiative forcing (Hansen *et al* 2005, Myhre *et al* 2013).

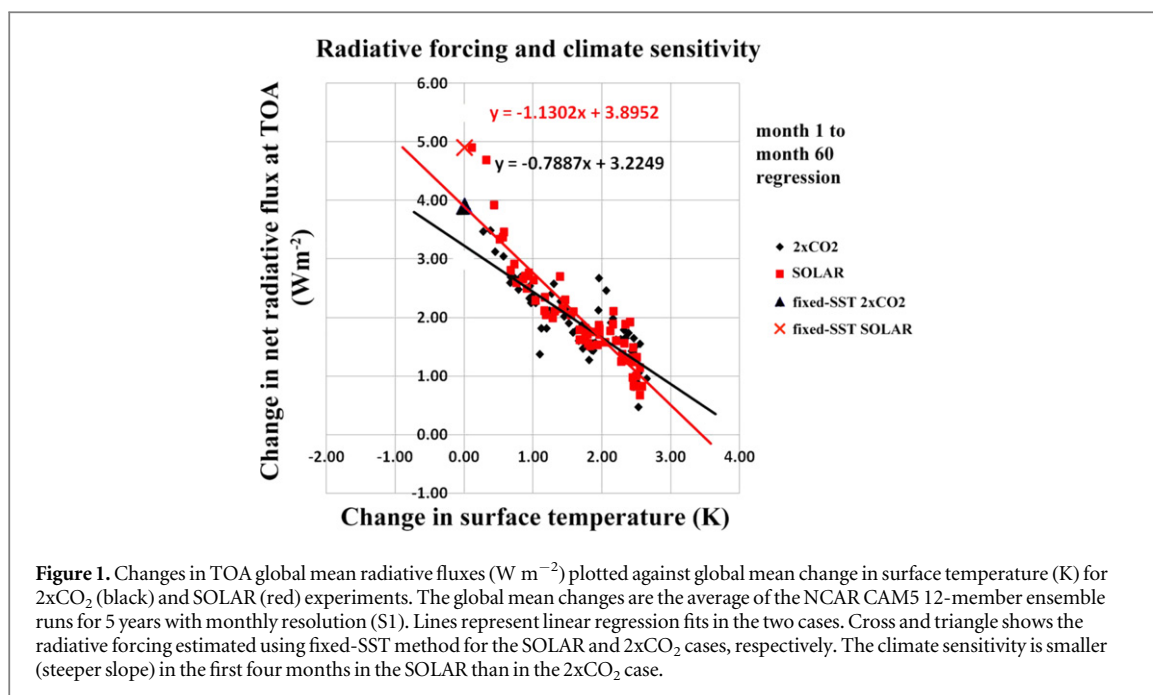
The SOM simulations are run for 100 years and the last 50 years are used for estimating the long term climate change. In both the configurations, monthly mean output is saved. In addition to these single member long-term simulations, we have also performed 5 year 12-member ensemble simulations for each of the three cases: each ensemble member is initialized from the start of different months (1st January, 1st February, and so on). The output from these ensemble simulations are saved in two different time periods, (i) daily mean output saved for 4 months and (ii) monthly mean output saved for 5 years. Averaging these 12 members produce annual mean data at monthly or daily time scales (Doutriaux-Boucher *et al* 2009) which enables us to have more data points for regression in the 5 years or in the 4 months after the instantaneous increase in  $\text{CO}_2$  concentration or solar irradiance. The 12-member ensemble simulations are initialized from the monthly restarts of the 100th year of the control simulation ('CTL').

Increased atmospheric  $\text{CO}_2$  concentration has a direct physiological effect on the opening of the plant stomata (Betts *et al* 2007, Doutriaux-Boucher *et al* 2009, Cao *et al* 2010) in addition to its radiative effect on the climate system. To estimate the contribution of  $\text{CO}_2$  radiative effect only, we performed another simulation in which the  $\text{CO}_2$  concentration is doubled (569.4 ppmv) only in the atmosphere model while the  $\text{CO}_2$  concentration in the land model is same as in the CTL (284.7 ppmv). This simulation, called '2x $\text{CO}_2$ rad', is again performed both in fixed-SST (40 years run) and SOM (100 years run) configurations. The 12-member ensemble simulations initialized from each month of the year is also performed in this case. We estimate the  $\text{CO}_2$  radiative effect by subtracting the CTL case from 2x $\text{CO}_2$ rad case while the  $\text{CO}_2$  physiological effect can be obtained by subtracting the 2x $\text{CO}_2$ rad case from 2x $\text{CO}_2$  case.

## 3. Results

### 3.1. Global mean response

We simulate a global mean surface warming of 4.1 K in 2x $\text{CO}_2$  and SOLAR simulations which is consistent with a climate sensitivity (global mean warming for a doubling of  $\text{CO}_2$ ) of  $\sim 4$  K for CAM5 (figure S1; Gettelman *et al* 2012). Table S4 shows the global, land and ocean mean changes in several key climate variables. In agreement with previous studies (Bala *et al* 2010, Cao *et al* 2011, 2012), we find that the global mean precipitation increases more due to the solar forcing (10.5%) than due to an equivalent increase in atmospheric  $\text{CO}_2$  (7.9%; figure S1, table S4). The difference in the precipitation response is a manifestation of the difference in the fast adjustments of the troposphere to the two forcings (Andrews *et al* 2009, Bala *et al* 2010, Cao *et al* 2012). Within the first month after  $\text{CO}_2$  is doubled, the stability of the lower



troposphere increases over ocean resulting in a decreased precipitation (figure S2, Cao *et al* 2012). Over land the fast surface warming acts to increase evaporation and precipitation (figure S3) but the  $\text{CO}_2$  physiological effect (caused by the closure of stomata, discussed later in detail) reduces the evapotranspiration (figure S4) which leads to decreased mean precipitation over land (figure S2, Cao *et al* 2012). In the SOLAR case, the atmospheric stability increases over ocean but to a much smaller magnitude compared to the  $\text{CO}_2$  forcing case and over land the physiological effect is absent. This results in a much smaller magnitude of the fast response global mean precipitation decrease (figure S2). Some studies (Held and Soden 2006, Bala *et al* 2008, Pendergrass and Hartmann 2014) have used the atmospheric energy balance perspective to explain the suppression of precipitation for  $\text{CO}_2$  forcing.

To estimate the radiative forcing, we use the average of the 12-member ensemble data from the  $2x\text{CO}_2$  and SOLAR experiments and adopt the Gregory method (figure 1, Gregory *et al* 2004). From the regression of 5 years of annual data at monthly intervals, we find that the regressed radiative forcing of  $2x\text{CO}_2$  and SOLAR is  $3.2 \text{ W m}^{-2}$  and  $3.9 \text{ W m}^{-2}$ , respectively (figure 1). We have used high time resolution for the first 5 years to capture the differing slopes in the two cases. We note that for the same long term global mean surface warming (4.1 K), the radiative forcing, estimated by the Gregory method (Gregory *et al* 2004), is larger in the SOLAR case. This is likely due to the differing adjustments in the first four months when the slope of the regression line which represents the net climate feedback for a forcing agent is steeper in the SOLAR case (figure 1). We estimate that the efficacy of the solar forcing is  $\sim 80\%$  from the regression method.

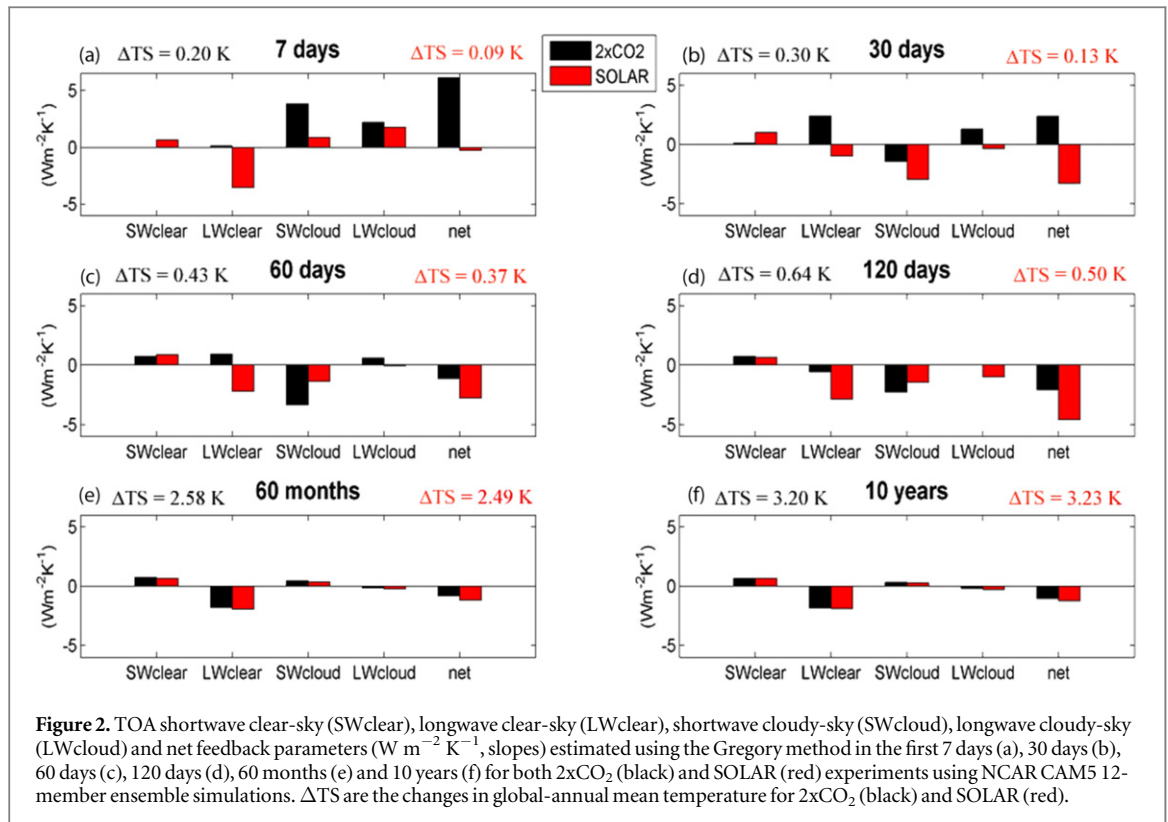
As discussed in the subsequent sections, we apply the regression method to 7, 30, 60 and 120 day periods and show that the rapid cloud response to the two forcings is responsible for smaller efficacy of solar forcing. Our estimate of the efficacy is within the range of results reported in a few past modeling studies (table S1).

### 3.2. Radiative forcing from the fixed-SST method

Another method of estimating the radiative forcing is the Hansen's fixed-SST method (Hansen *et al* 2005). Fixed-SST radiative forcing is defined as the net radiative flux change at the TOA after the forcing agent is introduced with the SST and sea-ice fixed (Hansen *et al* 2005). We find that the radiative forcing of  $2x\text{CO}_2$  and SOLAR estimated from the fixed-SST method is  $3.9 \text{ W m}^{-2}$  and  $4.9 \text{ W m}^{-2}$ , respectively (figure 1). Interestingly, we note that for the same long term global mean surface warming (4.1 K), the radiative forcing estimated by the fixed-SST method is also larger in the case of SOLAR. Further, our finding that the forcing in the fixed-SST method is larger than from the regressed radiative forcing is consistent with previous studies (Gregory and Webb 2008, Bala *et al* 2010, Andrews *et al* 2012). The monsoonal-type circulation changes associated with land warming, which is a fast adjustment, in the fixed-SST method is likely to lead to an incremental positive longwave cloud radiative forcing as discussed later.

### 3.3. Tropospheric adjustments in different time periods

Figure 2 shows the feedback parameters associated with shortwave clear-sky (SWclear), longwave clear-sky (LWclear), shortwave cloudy-sky (SWcloud) and longwave cloudy-sky (LWcloud) components and the net feedback parameter in time periods of 7 days, 1



month, 2 months, 4 months, 5 years and 10 years. A brief description of the method used to estimate the feedback parameters in these time periods is given in the supplemental material (S1). Figures S5 and S6 shows the contribution of land and ocean domains to these feedback parameters. These parameters are estimated as the slopes of the regression between the changes in the specific radiative flux component and changes in the global mean surface temperature (figure S7). Unless specified, the changes discussed here, are relative to the control experiment.

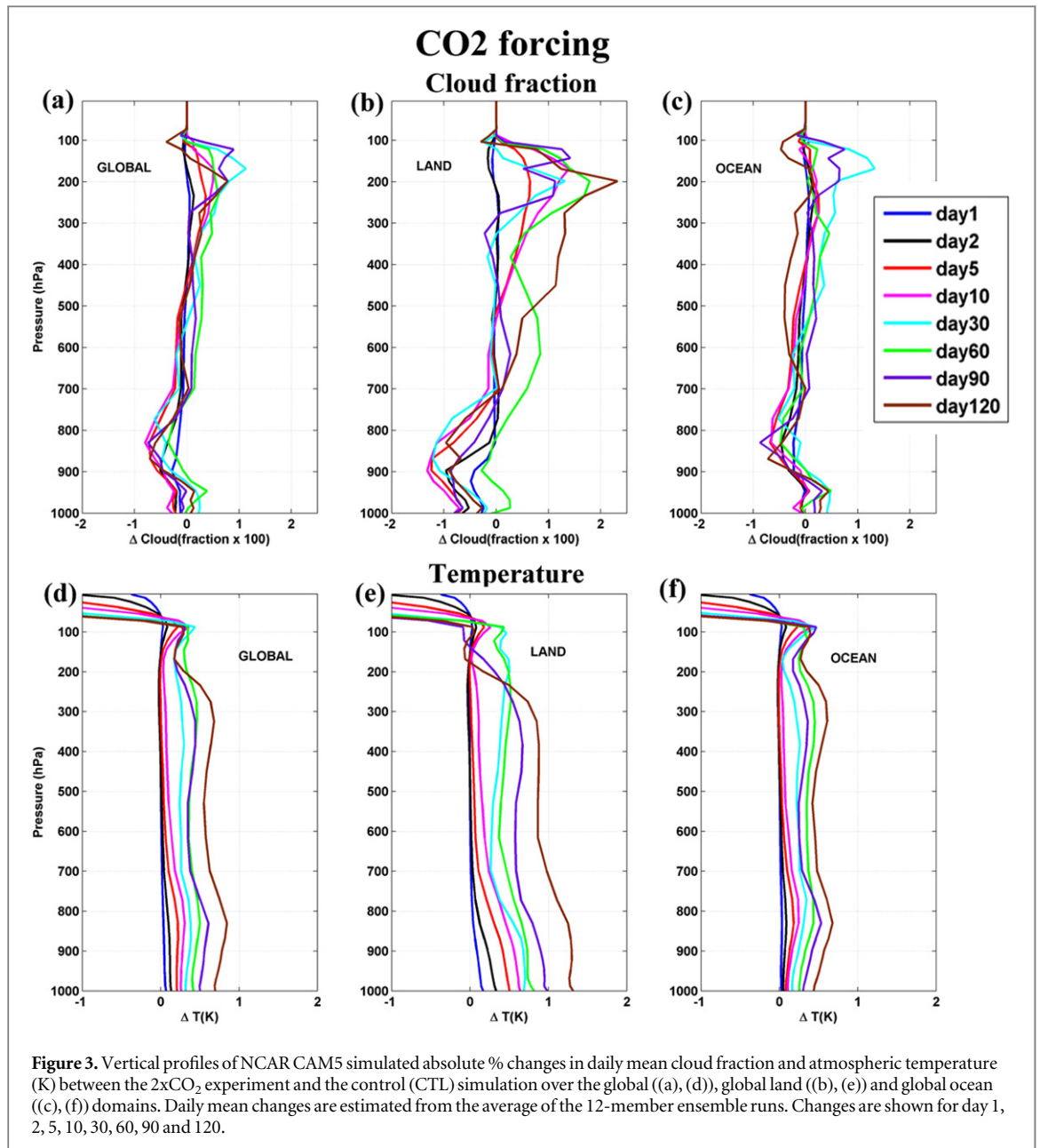
### 3.3.1. The first 7 days: cloud adjustment dominates

In the first 7 days, in the 2xCO<sub>2</sub> case, we find a strong net positive feedback (figure 2(a)). We find that the positive SWcloud and LWcloud feedbacks primarily contribute to the net feedback in our model simulations. This indicates that substantial cloud adjustments take place within the first 7 days after the forcing is imposed. The difference in the first 7 days response between a past study (Kamae and Watanabe 2012) where the positive LWclear feedback governs the net feedback on this timescale and our results could be because the climate model and the simulation configuration used in Kamae and Watanabe (2012) is different from the model and the simulation configuration used here.

We find that the low clouds decrease from day 1 over land (figure 3) as found in a recent study (Kamae and Watanabe 2012). We infer that the reduction of the low clouds over land is associated with the CO<sub>2</sub> physiological effect (Betts *et al* 2007, Doutriaux-

Boucher *et al* 2009, Bala *et al* 2010, Cao *et al* 2010, Andrews *et al* 2011, Cao *et al* 2012) because we find that the low clouds do not decrease over land when only the CO<sub>2</sub> radiative effect is considered (figure S8). In the 2xCO<sub>2</sub> case, the plant stomatal conductance reduces which in turn leads to a decline in plant transpiration. Reduced plant transpiration causes decreased relative humidity and hence diminished low level cloudiness over land (Cao *et al* 2012, figures 3 and S9). It also reduces the evaporative cooling and hence causes rapid land surface warming ( $\sim 0.6$  K) within a week (figures S3 and S10). The land surface warming is also affected by the CO<sub>2</sub> radiative effect: increase in the downward longwave radiation due to the elevated atmospheric CO<sub>2</sub>. However, the land surface warms at a slower rate when only the CO<sub>2</sub> radiative effect is considered (figures S3 and S11).

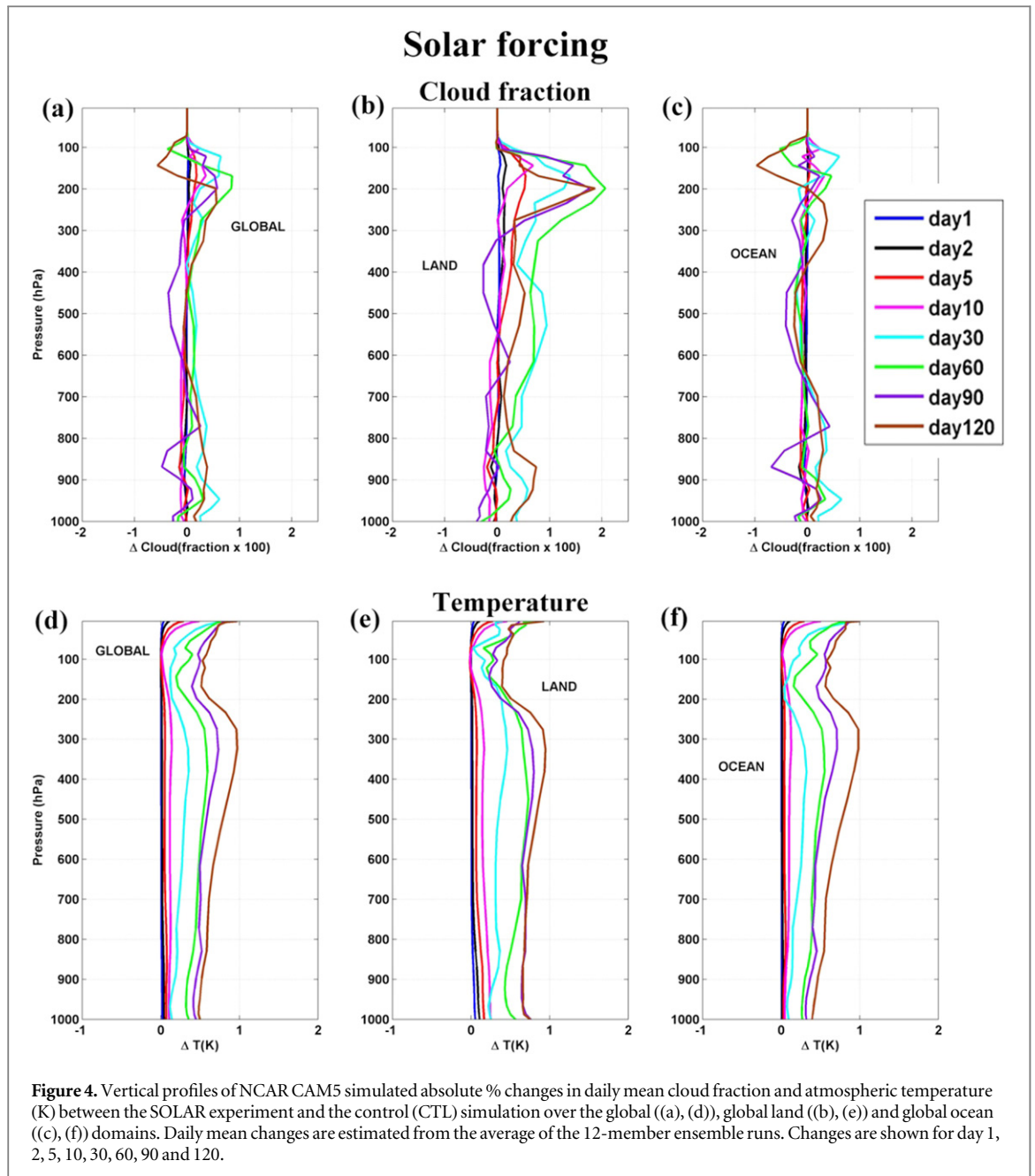
Owing to the large heat capacity of the ocean, the ocean surface temperature increases only slightly (figure S3) within the first week. As the land surface warms faster than the ocean, on day 1, 2 and 5 we find strong upward motion anomaly over land and corresponding downward motion anomaly over ocean (figure S12) resulting into a monsoonal-type of circulation (Cao *et al* 2012). Despite the upward motion over land we find reduced low clouds over land because the CO<sub>2</sub> physiological effect dominates. Reduced low clouds over land decreases the planetary albedo resulting in a positive SWcloud feedback (figure S5(a)) and this contribution dominates in the global mean (figure 2(a)). However, after 5 days we find that the high clouds increase over land in



association with increased relative humidity and enhanced updraft (figures 3 and S12, table S5). Increased high clouds over land results in a reduction of outgoing longwave radiation (OLR) and a strong positive LWcloud feedback (figure S5(a)) and this contribution dominates in the global mean (figure 2(a)). A combination of an increase in high clouds and a reduction in low clouds over land result in net positive cloud feedback in the 2xCO<sub>2</sub> case (figure S5(a)). We note that the cloud feedbacks over ocean have opposite sign to that over land but are weaker (figure S5(a)).

Similar to the 2xCO<sub>2</sub> case, we find that within day 5 the high clouds start to increase (figure 4, table S5) over land in the SOLAR case as well due to the enhanced upward motion (figure S12) which leads to a positive LWcloud feedback over land (figures 2(a) and S6(a)). However, over ocean we find that the LWcloud

feedback to be of opposite sign and relatively weaker (figure S6(a)). Thus, the overall LWcloud feedback is positive as it is dominated by the positive LWcloud feedback over land (figures 2(a) and S6(a)). From figure 2(a) we find that, in this 7-day period the net climate feedback is small as the positive LWcloud feedback is mostly offset by a large negative LWclear feedback. The strong negative LWclear feedback is because of the rapid stratospheric warming due to the shortwave absorption by ozone, water vapor and CO<sub>2</sub> (Manabe and Strickler 1964) which increases the OLR and consequently enhances the cooling rate. In summary, in first one week period, there is a strong net positive feedback in the 2xCO<sub>2</sub> case (mainly due to both SWcloud and LWcloud feedbacks associated with the cloud adjustments over land) and a slight net negative feedback in the SOLAR case (positive LWcloud feedback offsets negative LWclear feedback).



### 3.3.2. The first 30 days: transition to stratospheric and land-surface adjustment

By 30 days, there is an overlap of adjustment processes that dominate the first 7 day and the first 120 day time period. Here, we discuss this transition in detail. In the first 30-day time period, we find a net positive feedback in the  $2xCO_2$  case but a net negative feedback in the SOLAR case (figure 2(b)). In the  $2xCO_2$  case, the stratosphere cools during this period which leads to a decrease in OLR and hence a positive LWclear feedback. The low cloud cover continues to decrease over the land but over the ocean the low clouds, especially below 900 hPa, increase in association with an increase in near surface relative humidity. The increase in the near surface relative humidity is because of the increased stability over ocean (figures 3 and S9) which restricts vertical moisture transport out of the

boundary layer (Bala *et al* 2010, Cao *et al* 2012). We find a reduction in relative humidity at around 800–900 hPa and consequently less cloudiness at that level in the  $2xCO_2$  case (figures 3 and S9). The increase in the near-surface clouds causes a negative SWcloud feedback (figures 2(b) and S5(b)). However, during this 30 days we find that the high clouds over land continue to increase in association with the increased instability (figure 3) and increased updraft (figure S12). This contributes to a positive LWcloud feedback in the  $2xCO_2$  case (figures 2(b) and S5(b)). In the case of  $2xCO_2$ rad, the instability increases to a much smaller extent due to the absence of  $CO_2$  physiological effect (figure S8).

The net negative feedback in the SOLAR case is mainly due to the SWcloud feedback (figure 2(b)) as the cloud fraction over land increases throughout the

troposphere within 30 days (figure 4, table S5). Evapotranspiration over land increases with a gradual increase in the temperature in the SOLAR case (figures S3, S4 and S13), which results in a substantial increase in the specific humidity of the troposphere (figure S14). Further, similar to  $2\times\text{CO}_2$  case, the rapid land surface warming relative to ocean (figures S3 and S13) leads to a monsoonal-type of circulation evident from enhanced upward motion over land and consequently downward motion over ocean (figure S12). However, in the case of SOLAR, land surface warms at a slower rate compared to  $2\times\text{CO}_2$  (figures S3, S10 and S13). The monsoonal-type of circulation results in an inflow of water vapor from the ocean to land increasing the specific humidity of the troposphere over land (figure S14). The relative humidity also increases throughout the troposphere over land which results in an increased tropospheric cloud fraction (figure S14, figure 4 and table S5). However, over ocean due to marginal change in the stability (figure 4) there is little change in the cloud throughout the troposphere (figure 4). The elevated cloud fraction over land increases the planetary albedo and leads to a strong negative SWcloud feedback over land (figure S6(b)) which dominates the overall SWcloud feedback (figure 2(b)). As the high clouds continue to increase over land we find a positive LWcloud feedback over land which is offset by the negative LWcloud feedback over ocean (figures 2(b) and S6(b)). We note that in this 30 day period, the cloud feedbacks in both  $2\times\text{CO}_2$  and SOLAR cases are dictated by the cloud adjustments over land. Overall, it is important to note that the LWclear and SWcloud feedbacks combine to produce a positive feedback in the  $2\times\text{CO}_2$  case but negative feedback in the SOLAR case (figure 2(b)).

### 3.3.3. Adjustments in the first 4 months: stratospheric and land-surface adjustments

The net feedback is negative in both  $2\times\text{CO}_2$  and SOLAR cases in the 2 and 4 month periods (figure 2(c)) but the magnitude is much larger in the SOLAR case. The LWclear and SWcloud feedbacks mainly dictate the net feedback (figures 2(c) and (d)) in both cases. In the SOLAR case, the LWclear and SWcloud feedbacks are negative and combine to produce a strong net negative feedback while in the  $2\times\text{CO}_2$  case, the LWclear feedback *offsets or adds slightly* to the negative SWcloud feedback resulting in a relatively smaller net negative feedback. As discussed in earlier sections, the negative LWclear feedback in the case of SOLAR is associated with the stratospheric warming while the stratospheric cooling causes a positive LWclear in the  $2\times\text{CO}_2$  case. The negative SWcloud feedback in both cases is due to enhanced cloud fraction over land (figures 3 and 4, table S5). This is further evident from the figures S5(c) and S6(c) which shows the dominance of SWcloud feedback over land.

In this 2–4 month period, in both  $2\times\text{CO}_2$  and SOLAR cases, the temperature of the whole troposphere increases (figures 3 and 4) which in turn increases the specific humidity of the troposphere (figures S9 and S14). We find an increase in relative humidity (figures S9 and S14) and hence an increase in the cloud fraction leading to a negative SWcloud feedback in both cases (figure 4). The reinforcement of LWclear and SWcloud feedbacks to produce a strong net negative feedback in the case of SOLAR is the cause for requiring a larger solar radiative forcing for the same long term climate warming.

In both  $2\times\text{CO}_2$  and SOLAR cases, the weakening of the land-sea contrast and hence the monsoonal-type circulation during the 60 and 120 day time periods relative to the 7 and 30 day time periods can be seen (figures S10–13). As a result, we find that the cloud feedbacks mainly over land start to weaken (figures S5(d) and S6(d)), and the clear-sky feedbacks start to dominate the cloud feedbacks in both the cases. The weaker cloud feedbacks and the dominance of clear-sky feedbacks after 4 months indicate that the timescale for the dominance of rapid land adjustment and the associated monsoonal-type circulation in this model is approximately 4 months.

### 3.3.4. Adjustment on the decadal timescale: ocean mixed-layer adjustment

The feedbacks after 4 months represent the feedbacks associated with the mixed layer ocean adjustment that lasts for a few decades (figures 2(e) and (f)). However, in simulations with representations of deep ocean processes, this adjustment would extend out over many centuries (Gregory *et al* 2004). As is well known, we find that the net feedback is negative in the 5–10 year time period for both  $2\times\text{CO}_2$  and SOLAR cases but it is larger in the SOLAR case (figures 2(e) and (f)). In our simulations, the negative LWclear feedback mainly drives the net feedback in both the cases. By the end of 10 years, the global mean surface temperature reaches ~80% of the equilibrium global mean warming. In this longer time period, we find that the cloud feedbacks are too small and it is the clear-sky feedbacks that mainly contribute to the net feedback (figures 2(e) and (f)). This indicates that the cloud feedbacks are important on the fast timescales as found in other recent studies (Gregory and Webb 2008, Bala *et al* 2010, Kamae and Watanabe 2012). However, they do play a significant role in shaping the long term climate response (Gregory and Webb 2008, Bala *et al* 2010, Kamae and Watanabe 2012).

In the mixed layer ocean time period which extends out to decades it is likely that the changes in the spatial pattern of SST and ocean heat uptake could influence the radiative forcing and the climate feedback parameters (Armour *et al* 2013, Andrews *et al* 2015, Cao *et al* 2015). Further, on centennial time scales, the feedbacks from deep ocean changes, ocean heat uptake and biogeochemical cycle could cause

changes to these parameters (Cao *et al* 2015, Knutti and Rugenstein 2015).

#### 4. Results from HadCM3L

To demonstrate the robustness of the mechanism discussed here that the rapid cloud and stratospheric adjustments in the first 4 month period is responsible for the lower efficacy of solar forcing, we now discuss results from UK Met Office Hadley Centre global climate model HadCM3L (Cao *et al* 2012; S2).

We find that the long term global mean warming due to quadrupled CO<sub>2</sub> and 4% increased solar constant is 5.71 K and 5.70 K, respectively while the radiative forcing estimated from the Gregory method (Gregory *et al* 2004) is 7.9 W m<sup>-2</sup> and 8.8 W m<sup>-2</sup>, respectively (figure S15). Thus, we find that for the same global mean equilibrium surface warming, the difference between the CO<sub>2</sub> and solar forcing in this model is ~1 W m<sup>-2</sup> which is consistent with the results from the NCAR CAM5 simulations. The efficacy of solar forcing estimated from HadCM3L is ~89%. As for NCAR CAM5, we find that the slope of the regression line which represents the net climate feedback is steeper in the first four months in case of solar forcing than CO<sub>2</sub> forcing in HadCM3L (figure S15). This indicates the robustness of the results from NCAR CAM5 discussed above. A detailed discussion on the consistency between the results from HadCM3L and NCAR CAM5 is in S3.

#### 5. Discussion and conclusion

In this paper, using NCAR CAM5 model simulations, we have examined the physical mechanisms associated with the lower efficacy for solar forcing compared to an equivalent CO<sub>2</sub> forcing. For the same equilibrium global mean surface warming (~4.1 K), we find that the efficacy of solar forcing is ~80%. Previous studies (Andrews *et al* 2009, Bala *et al* 2010, Cao *et al* 2012) have indicated that the differences in the rapid climate response could lead to major differences in the total climate response. In this study, we provide a systematic investigation of how the feedback mechanisms associated with fast adjustment which includes rapid changes in clouds and stratospheric thermal structure and land surface adjustments could lead to smaller efficacy for solar forcing. A schematic illustration of the rapid tropospheric adjustments over land and ocean for the 2xCO<sub>2</sub> and SOLAR cases in 7 day, 30 day and 120 day time periods is shown in figure 5. Figure S16 summarizes the net feedbacks on 7 day, 30 day, 60 day, 120 day, 60 month and 10 year time periods.

Our study indicates that the total climate response in the slab ocean CAM5 model simulations can be characterized by three time periods: (i) first 7 days time period (ultrafast response), where the net feedback in the 2xCO<sub>2</sub> case is positive while it is negative in the

SOLAR case (figure 2(a)), (ii) 4 month time period (fast response) when the net feedback is negative in both cases but the magnitude is larger in the SOLAR case (figures 2(c) and (d)), and (iii) 5–10 year time period (slow response) which is the mixed-layer ocean adjustment time period, where the net feedback is negative in both cases and is dominated by LWclear feedbacks (figures 2(e) and (f)). Transitions between these time periods represent transitions between processes that dominate changes in the relationship between top-of-atmosphere fluxes and global mean near-surface air temperatures.

Our study shows that in the first four months period in the SOLAR case, the cloud fraction increases mainly over land which enhances the planetary albedo which in turn leads to a strong negative SWcloud feedback. This SWcloud feedback combines with the negative LWclear feedback due to stratospheric warming producing a strong net negative feedback. In the 2xCO<sub>2</sub> case too, the tropospheric cloud fraction increases which leads to a negative SWcloud feedback. However, this is offset by a positive LWclear feedback due to stratospheric cooling producing a smaller net negative feedback. The stronger net negative feedback (steeper slope of the Gregory regression line) in case of solar forcing, relative to CO<sub>2</sub> forcing, necessitates a larger radiative forcing for the same long term warming and hence an efficacy less than one. Because the slope is larger in the first 4 months, its influence is seen even when the regression is extended to, for example, 5 years (figure 1). In the absence of CO<sub>2</sub> physiological effect, it is likely that the fast cloud adjustments would not be very different between the SOLAR and 2xCO<sub>2</sub> case. Hence, the major cause for the differing efficacies is the differing stratospheric response in the first few months: warming in case of SOLAR and cooling in case of 2xCO<sub>2</sub>.

Other factors could also influence the magnitude of efficacy. For instance, Hansen *et al* (1997) and Forster *et al* (2000) find that a radiative forcing at low latitudes could lead to a smaller efficacy than a forcing at high latitudes because of sea ice albedo feedback and more stable lapse rate at high latitudes which causes confinement of warming closer to the surface. A forcing at low latitudes could also lead to larger negative temperature feedback as the temperatures are larger there. In the case of solar forcing which affects the tropics more than the high latitudes, these effects could also partly contribute to the smaller efficacy of solar forcing in addition to the mechanism described above.

The Gregory method does have limitations because it relies on linear regression for describing climate change over a range of timescales. The magnitude of the estimated efficacy would depend on the time resolution of the data used for regression and the total time period of the data. For example, the smaller efficacy of solar forcing is discernable easily when data at monthly interval is plotted in figure 1. However, when data at yearly interval is used, the linear

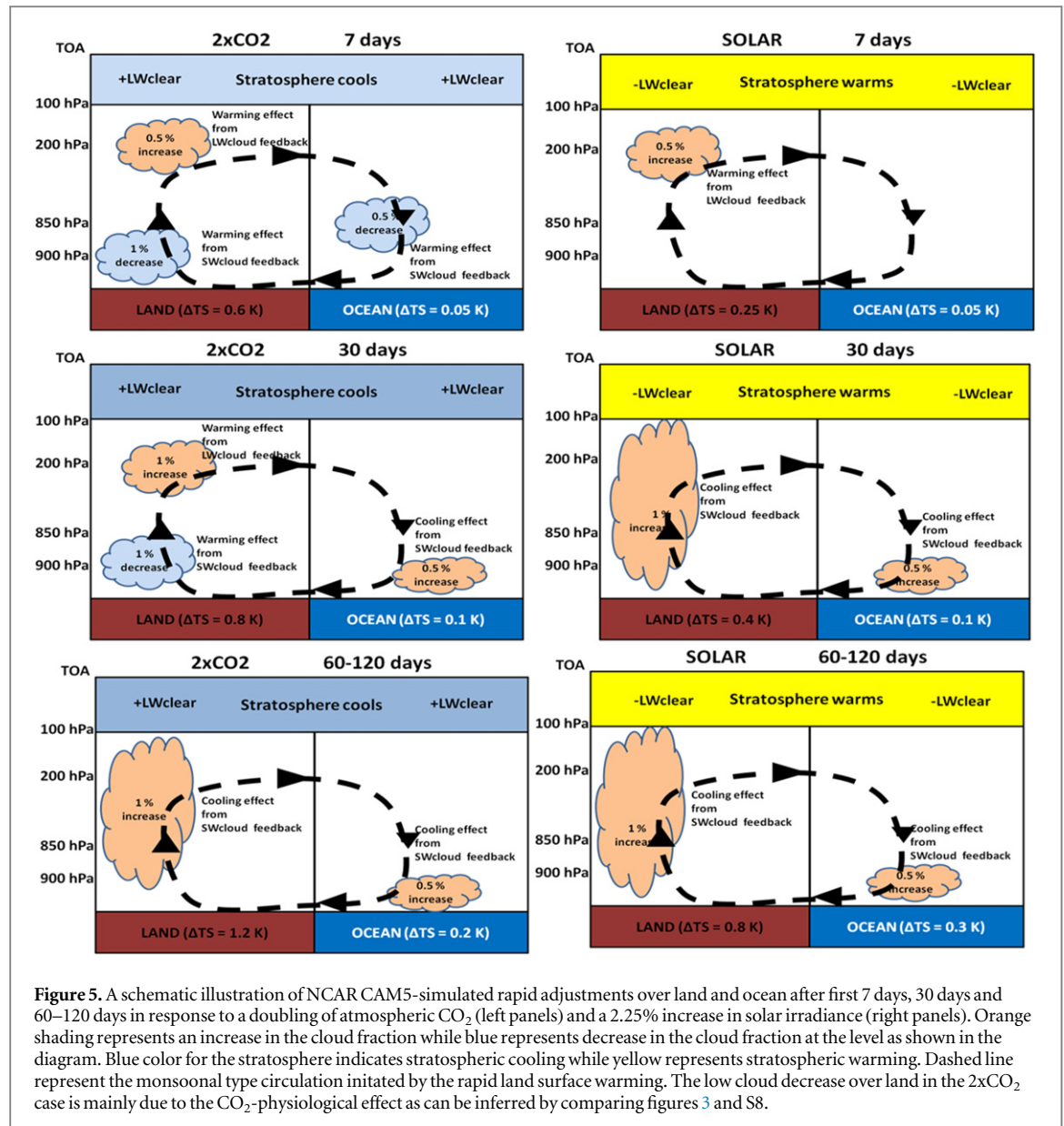


**Figure 5.** A schematic illustration of NCAR CAM5-simulated rapid adjustments over land and ocean after first 7 days, 30 days and 60–120 days in response to a doubling of atmospheric  $\text{CO}_2$  (left panels) and a 2.25% increase in solar irradiance (right panels). Orange shading represents an increase in the cloud fraction while blue represents decrease in the cloud fraction at the level as shown in the diagram. Blue color for the stratosphere indicates stratospheric cooling while yellow represents stratospheric warming. Dashed line represent the monsoonal type circulation initiated by the rapid land surface warming. The low cloud decrease over land in the  $2\times\text{CO}_2$  case is mainly due to the  $\text{CO}_2$ -physiological effect as can be inferred by comparing figures 3 and S8.

regression would not adequately capture the differing fast adjustment and hence the estimated efficacy could be larger. Similarly, when more than 10 years of data are used the estimated efficacy is larger—when annual mean data for 70 and 100 years are used, we found that estimated efficacy is 0.92 and 0.96, respectively, as the slopes are strongly influenced by slow response which is nearly the same for SOLAR and  $2\times\text{CO}_2$ .

Investigation of the climate system's response to various radiative forcing agents is of practical relevance as it aids in assessing and comparing the climate impact of different forcing agents. As discussed in several previous studies (Bala *et al* 2010, Cao *et al* 2012, Kamae and Watanabe 2012) it is important to separate out the fast effects on atmospheric structure from the effects resulting from gradual planetary warming. Here, we have shown that understanding the tropospheric adjustments in a time period beyond one week but within 4 months period is necessary to completely

understand the efficacy of solar forcing. Though in our study we impose idealized abrupt forcings of carbon dioxide and solar irradiance, any continuous time series of radiative forcing changes can be considered as a convolution of infinitesimal step-function changes (Good *et al* 2011). Therefore, the conclusions drawn in this study also apply to continuous changes in radiative forcing. The results from this study is from simulations using two climate models: a slab ocean model (NCAR CAM5) and an atmosphere-ocean coupled general circulation model (HadCM3L). Further studies involving multiple models would be useful to test the robustness of our results.

The results presented here indicate that the fast response could have important implications for the efficacy of various forcing agents. In this work, we have considered the simple case of solar irradiance change. Other forcing agents such as aerosols could have much more complex fast interaction with clouds by acting as

cloud condensation nuclei or by warming the cloud environment in the case of black carbon (e.g. Xu and Xie 2015). The importance of fast cloud response in the case of black carbon aerosols is highlighted by a past study (Ban-Weiss *et al* 2011) which shows that the variation in climate response from black carbon at different altitudes occurs largely from different fast climate responses and temperature-dependent slow responses are indistinguishable.

Given the climate system's response to CO<sub>2</sub> forcing, our study could help to interpret past climatic changes such as during the Maunder minimum (1645–1715, Eddy 1976) when the solar irradiance was less ( $-0.32 \text{ W m}^{-2}$ ) and the associated global mean cooling was 0.3–0.4 K (Shindell *et al* 2001) relative to late 18th century. Our results also have direct relevance to improved estimates of the climate response due to major volcanic eruptions such as Mount Pinatubo, 1991 which caused a global mean cooling of about 0.5 K in the year following eruption (McCormick *et al* 1995). As in the case of increased solar irradiance, the heating of the stratosphere by aerosols is likely to result in smaller efficacy for volcanic forcing. Niemeier *et al* (2013) show that the stratospheric aerosol forcing must be larger than solar forcing to achieve the same surface temperature change. Further, our results also have implications for estimating the amount of reduction in solar absorption that is required in the solar radiation management (SRM) geoengineering methods (Schmidt *et al* 2012). In agreement with our study, it has been found that the solar irradiance reduction needed to offset the warming from quadrupling CO<sub>2</sub> forcing is larger by about 20% in that study (Schmidt *et al* 2012).

In summary, our study shows that in the first four months the negative LWclear and SWcloud feedbacks combine to produce a strong net negative feedback in the SOLAR case while in the 2xCO<sub>2</sub> case, the LWclear feedback offsets or adds slightly to the negative SWcloud feedback resulting in a relatively smaller net negative feedback. The larger negative feedback (steeper slope of the regression line) in case of SOLAR relative to 2xCO<sub>2</sub> forcing, necessitates a larger radiative forcing (larger intercept) for the same equilibrium surface warming and hence a lower efficacy for solar forcing.

## Acknowledgments

We thank Mr Lei Duan and Miss Wei Liu for drafting the illustrations from the HadCM3L model simulations. CAM5 simulations were performed out at Centre for Atmospheric and Oceanic Sciences High Performance Computing facility funded by Fund for Improvement of S & T Infrastructure, Department of Science and Technology.

## References

- Andrews T, Doutriaux-Boucher M, Boucher O and Forster P M 2011 A regional and global analysis of carbon dioxide physiological forcing and its impact on climate *Clim. Dyn.* **36** 783–92
- Andrews T, Forster P M and Gregory J M 2009 A surface energy perspective on climate change *J. Clim.* **22** 2557–70
- Andrews T, Gregory J M and Webb M J 2015 The dependence of radiative forcing and feedback on evolving patterns of surface temperature change in climate models *J. Clim.* **28** 1630–48
- Andrews T, Gregory J M, Webb M J and Taylor K E 2012 Forcing, feedbacks and climate sensitivity in CMIP5 coupled atmosphere-ocean climate models *Geophys. Res. Lett.* **39** L09712
- Armour K C, Bitz C M and Roe G H 2013 Time-varying climate sensitivity from regional feedbacks *J. Clim.* **26** 4518–34
- Bala G, Caldeira K and Nemani R 2010 Fast versus slow response in climate change: implications for the global hydrological cycle *Clim. Dyn.* **35** 423–34
- Bala G, Duffy P B and Taylor K E 2008 Impact of geoengineering schemes on the global hydrological cycle *Proc. Natl Acad. Sci. USA* **105** 7664–9
- Ban-Weiss G A, Cao L, Bala G and Caldeira K 2011 Dependence of climate forcing and response on the altitude of black carbon aerosols *Clim. Dyn.* **38** 897–911
- Betts R A *et al* 2007 Future runoff changes due to climate and plant responses to increasing carbon dioxide *Nature* **448** 1037–42
- Cao L, Bala G and Caldeira K 2011 Why is there a short-term increase in global precipitation in response to diminished CO<sub>2</sub> forcing? *Geophys. Res. Lett.* **38** L06703
- Cao L, Bala G and Caldeira K 2012 Climate response to changes in atmospheric carbon dioxide and solar irradiance on the time scale of days to weeks *Environ. Res. Lett.* **7** 034015
- Cao L, Bala G, Caldeira K, Nemani R and Ban-Weiss G 2010 Importance of carbon dioxide physiological forcing to future climate change *Proc. Natl Acad. Sci. USA* **107** 9513–8
- Cao L, Bala G, Zheng M and Caldeira K 2015 Fast and slow climate responses to CO<sub>2</sub> and solar forcing: a linear multivariate regression model characterizing transient climate change *J. Geophys. Res. Atmos.* **120** 12037–53
- Dong B W, Gregory J M and Sutton R T 2009 Understanding land-sea warming contrast in response to increasing greenhouse gases: I. Transient adjustment *J. Clim.* **22** 3079–97
- Doutriaux-Boucher M, Webb M J, Gregory J M and Boucher O 2009 Carbon dioxide induced stomatal closure increases radiative forcing via a rapid reduction in low cloud *Geophys. Res. Lett.* **36** L02703
- Eddy J A 1976 The maunder minimum *Science* **192** 1189–202
- Forster P M, Andrew T, Good P, Gregory J M, Jackson L S and Zelinka M 2013 Evaluating adjusted forcing and model spread for historical and future scenarios in the CMIP5 generation of climate models *J. Geophys. Res.: Atmos.* **118** 1139–50
- Forster P M F, Blackburn M, Glover R and Shine K P 2000 An examination of climate sensitivity for idealised climate change experiments in an intermediate general circulation model *Clim. Dyn.* **16** 833–49
- Gottelman A, Kay J E and Shell K M 2012 The evolution of climate sensitivity and climate feedbacks in the community atmosphere model *J. Clim.* **25** 1453–69
- Good P, Gregory J M and Lowe J A 2011 A step-response simple climate model to reconstruct and interpret AOGCM projections *Geophys. Res. Lett.* **38** L01703
- Gregory J and Webb M 2008 Tropospheric adjustment induces a cloud component in CO<sub>2</sub> forcing *J. Clim.* **21** 58–71
- Gregory J M *et al* 2004 A new method for diagnosing radiative forcing and climate sensitivity *Geophys. Res. Lett.* **31** L03205
- Hansen J, Sato M and Ruedy R 1997 Radiative forcing and climate response *J. Geophys. Res. Atmos.* **102** 6831–64
- Hansen J *et al* 2005 Efficacy of climate forcings *J. Geophys. Res. Atmos.* **110** D18104

- Held I M and Soden B J 2006 Robust responses of the hydrological cycle to global warming *J. Clim.* **19** 5686–99
- Held I M, Winton M, Takahashi K, Delworth T, Zeng F and Vallis G K 2010 Probing the fast and slow components of global warming by returning abruptly to preindustrial forcing *J. Clim.* **23** 2418–27
- Kamae Y and Watanabe M 2012 Tropospheric adjustment to increasing CO<sub>2</sub>: its timescale and the role of land–sea contrast *Clim. Dyn.* **41** 3007–24
- Knutti R and Rugenstein M 2015 Feedbacks, climate sensitivity, and the limits of linear models *Phil. Trans. R. Soc. A* **373** 20150146
- Lambert F H and Faull N E 2007 Tropospheric adjustment: the response of two general circulation models to a change in insolation *Geophys. Res. Lett.* **34** L03701
- Manabe S and Strickler R F 1964 Thermal equilibrium of the atmosphere with a convective adjustment *J. Atmos. Sci.* **21** 361–85
- McCormick M P, Thomason L W and Trepte C R 1995 Atmospheric effects of the Mt Pinatubo Eruption *Nature* **373** 399–404
- Myhre G *et al* 2013 Anthropogenic and natural radiative forcing *Climate Change 2013: The Physical Science Basis. Contribution of Working Group I to the Fifth Assessment Report of the Intergovernmental Panel on Climate Change* ed T F Stocker *et al* (Cambridge: Cambridge University Press)
- Neale *et al* 2010 Description of the NCAR community atmosphere model (CAM5.0) *NCAR Tech. Note NCAR/TN-4861STR* p 268 ([http://cesm.ucar.edu/models/cesm1.1/cam/docs/description/cam5\\_desc.pdf](http://cesm.ucar.edu/models/cesm1.1/cam/docs/description/cam5_desc.pdf))
- Niemeier U, Schmidt H, Alterskjær K and Kristjánsson J E E 2013 Solar irradiance reduction via climate engineering Impact of different techniques on the energy balance and the hydrological cycle *J. Geophys. Res.: Atmos.* **118** 11905–17
- Pendergrass A G and Hartmann D L 2014 The atmospheric energy constraint on global mean precipitation change *J. Clim.* **27** 757768
- Schmidt *et al* 2012 Solar irradiance reduction to counteract radiative forcing from a quadrupling of CO<sub>2</sub>: climate responses simulated by four earth system models *Earth Syst. Dynam.* **3** 63–78
- Shindell D T, Schmidt G A, Mann M E, Rind D and Waple A 2001 Solar forcing of regional climate change during the maunder minimum *Science* **294** 2149–52
- Staten P, Reichler T and Lu J 2014 The transient circulation response to radiative forcings and sea surface warming *J. Clim.* **7** 93239336
- Xu Y and Xie S P 2015 Ocean mediation of tropospheric response to reflecting and absorbing aerosols *Atmos. Chem. Phys.* **15** 5827–33